Catena 239 (2024) 107847

Contents lists available at ScienceDirect

Catena

journal homepage: www.elsevier.com/locate/catena

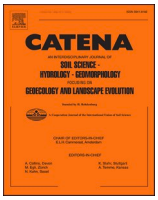

# Reconstructing historic bog iron ore deposits in the Bourtangermoor, a former raised bog in the Netherlands

Aukjen A. Nauta [a,*], Roel Dijksma [b], Jasper H.J. Candel [a], Cathelijne R. Stoof [c]

[a] Soil Geography and Landscape Group, Wageningen University, Wageningen, the Netherlands
[b] Hydrology and Quantitative Water Management Group, Wageningen University, Wageningen, the Netherlands
[c] Soil Physics and Land Management, Wageningen University, Wageningen, the Netherlands

ARTICLE INFO

*Keywords:*
Bog iron ores
Siderite
Raised bog
Seepage
Historic data

ABSTRACT

Bog iron ores are well-known lumps of Fe-(oxy)hydroxides (goethite, limonite) found along streams and in seasonally flooded, low-lying areas. Historic literature of the Bourtangermoor, a former raised bog in the north of the Netherlands and adjacent Germany, however, revealed a second, rare type of bog iron ores, exclusively composed of siderite (Fe-carbonate) with accessory vivianite (Fe-phosphate), minerals only stable under anaerobic conditions. In this research we compared historic literature and maps mainly from the first half of the 20th century, when parts of the bog were still intact, with present-day seepage data to allow analysis whether recent seepage could be used to reconstruct the location of historic bog iron ores in the Bourtangermoor. Our results showed two distinctly different present-day seepage patterns: one related to shallow aquifers, one to deeper aquifers. Present-day seepage from deeper aquifers was related to historic siderite bog iron ore deposits (deposits exclusively limited to the lower, early formed, still groundwater-fed part of the raised bog). Present-day seepage – deep or shallow – did not show a clear relation to historic classic-type bog iron ores (lumps of goethite and limonite). We conclude that present-day seepage patterns from deep aquifers can be used to reconstruct historic siderite bog iron ores in the Bourtangermoor. Present-day seepage patterns – deep or shallow – are however not representative for historic bog iron ores deposited along streams. Our results could be useful for wetland restoration projects as iron can contribute to nutrient-poor conditions by capturing phosphate in bog iron ores and for archaeological research regarding the potential use of bog iron ores by past societies.

## 1. Introduction

The Bourtangermoor in the north of the Netherlands and adjacent Germany (Fig. 1), was once part of the extensive raised bog belt in Northwest-Europe, extending from Ireland to Poland. Large parts – including the Bourtangermoor – have disappeared due to centuries of peat cutting, but some parts of the former Bourtangermoor still remain, for example nature reserve Bargerveen, which is the largest bog remnant of the Netherlands. Many of the still existing bogs are threatened by drainage and present-day peat cutting (Koster and Favier, 2005; Berendsen and Stouthamer, 2008). Wetlands are, however, an important landscape regarding water management (water retention and storage), biodiversity, climate change and $CO_2$-sequestration (Baird, 2009; Bragazza et al., 2009; Laine, 2009; Yu et al., 2009; McBratney et al., 2014; Nichols and Peteet, 2019). Nature restoration projects are established to conserve the remaining raised bog patches and restore former wetlands (Schouten, 2002; Bönsel and Sonneck, 2011; Mohr et al., 2015; Joosten et al., 2017; Chimner et al., 2017). Bog iron ores can contribute to the redevelopment of wetlands by their ability to incorporate phosphate in Fe-complexes and the mineral vivianite (Fe-phosphate), thus reducing the amount of nutrients in the environment (Heiberg et al., 2012; Aggenbach et al., 2013; Walpersdorf et al., 2013; Emsens et al., 2017). However, large amounts of iron in groundwater can be toxic to plants and can inhibit the growth of specific bog vegetation (Lucassen, 2000; Aggenbach et al., 2013). Furthermore, sheet-like bog iron ore deposits can impact local hydrological conditions as they can form an impermeable layer in the shallow subsurface (Anderson, 1962; Kaczorek and Sommer, 2004; Thelemann et al., 2017).

Lumps or thin sheets of iron(oxy)hydroxide (e.g. goethite, limonite) deposited along streams or in seasonally flooded low-lying areas – further referred to as classic-type bog iron ores – are well studied (Knibbe, 1969; Booy, 1986; Kaczorek et al., 2004). Their mineralogy and

* Corresponding author.
*E-mail address:* aukjen.nauta@wur.nl (A.A. Nauta).

https://doi.org/10.1016/j.catena.2024.107847
Received 10 August 2023; Received in revised form 16 January 2024; Accepted 21 January 2024
Available online 5 March 2024

chemical composition are well established (Schwertmann, 1992; Virtanen, 1994; Kaczorek and Sommer, 2004), as is their mode of deposition: reduction of iron in acid soils, leakage of iron into the shallow groundwater system, oxidization of iron when groundwater reaches the surface again, resulting in deposition of Fe-(oxy)hydroxides close to the surface with accessory siderite in the lower, water-saturated, reduced part of the soil (Knibbe, 1969; Casparie, 1972; Kaczorek and Sommer, 2004). Yet little is known about the impact of bog iron ores in groundwater-fed peat that later developed into a raised bog: the possible changes in their mineralogy during the development of the raised bog and their impact on early wetland development (Postma, 1980; Shotyk, 1988). The bog iron ores in the Bourtangermoor were composed exclusively of siderite with accessory vivianite (Van Bemmelen, 1895; Van Bemmelen et al., 1900; Reinders, 1902; Visscher, 1931; Casparie, 1972). They were unique in size with lenses up to 10 m in circumference and 2 m thick in a layer that could be followed for tens of meters. These deposits – further referred to as siderite bog iron ores – were formed under different geochemical conditions compared to their classical counterparts, as siderite ($Fe_2CO_3$) and vivianite ($[Fe_3(PO_4)_2{\cdot}8H_2O]$), can only be formed under reducing conditions (Postma, 1980; Schwertmann, 1992; Virtanen, 1994).

The Bourtangermoor bog iron ores could provide valuable information for archaeological research. Bog iron ores formed along streams were mined from prehistoric to recent times (Groenewoudt and van Nie, 1995; Thelemann et al., 2017). Little is known, however, about their possible use as a raw material in parts of the landscape associated with raised bogs (Jansen and Grootjans, 2019; Paulissen, 2023).

In this research, we investigated the hypothesis that present-day seepage could be used to reconstruct historic bog iron ore deposits and identify the mechanisms responsible for bog iron ore deposition in areas closely related to raised bogs. Understanding these mechanisms could be useful for restauration projects to assess the impact of bog iron ores on the early development of wetlands. We addressed the following research questions: (1) Where in the Bourtangermoor were bog iron ores found (both spatially and at what depth in peat profiles). (2) Can present-day seepage patterns explain the spatial distribution of siderite bog iron ore and classic-type bog iron ore? (3) Can siderite/vivianite deposits be regarded as the start of peat formation which eventually led to the creation of bogs.

## 2. Materials and methods

### 2.1. Study area

The study was done in the Dutch part of the Bourtangermoor, one of the largest raised bog systems in Northwest-Europe before large-scale

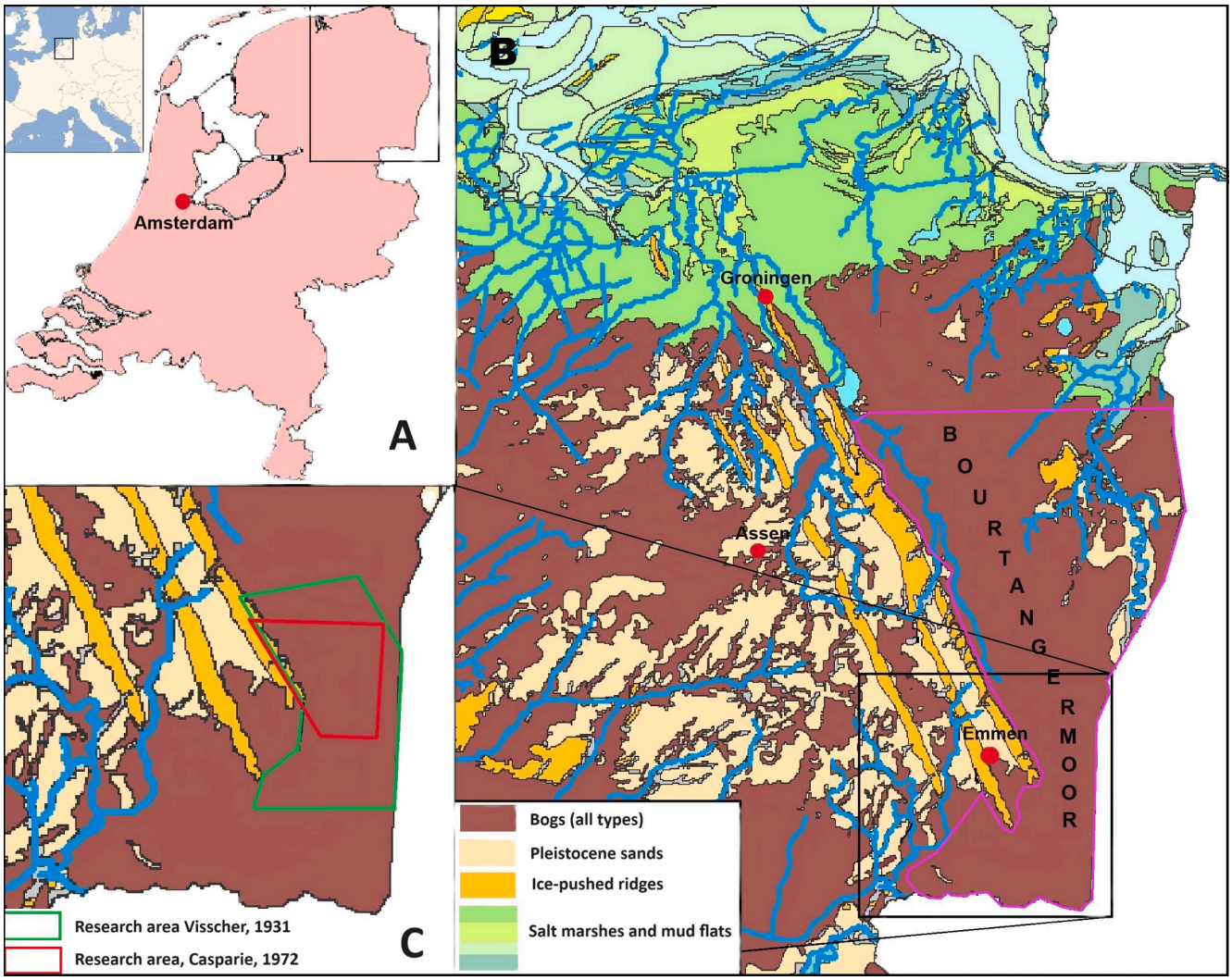


**Fig. 1.** (A) Location of the former raised bog Bourtangermoor in the north of the Netherlands. (B) Palaeogeographical map of 1500 CE, showing the maximum extent of bogs in the area (Vos et al., 2020). Pink boundary: extension of the Bourtangermoor. (C) Southern part of the raised bog with the research areas of the two historic dissertations used.

peat extraction (Casparie, 1972). It is situated in the north of the Netherlands and continues into Germany up to the river Ems (Fig. 1). The total area of the Bourtangermoor at its maximum extent was approximately 3000 $km^2$ (Casparie, 1972; Vos et al., 2020). Centuries of large-scale-peat cutting reduced the Bourtangermoor to only a few scattered raised bog patches. Nature reserve projects work at conservation of existing raised bog and restoration of former raised bog areas (e.g. Bargerveen in the Netherlands, Rühler Moor in Germany) (Jansen and Grootjans, 2019; Bourtangermoor, 2021; Stichting Bargerveen, 2021).

Bog development in the area started circa 7000 years BP in the area east of the Hondsrug (Jansen and Grootjans, 2019), a megaflute (glacial ridge) shaped during the second last ice age (Saalien, ca 150.000 years ago) when the northern part of the Netherlands was covered with ice (Berendsen and Stouthamer, 2008; Vos et al., 2020). After the retreat of the ice, the paleo-valley of the river Ems extended up to the Hondsrug, eroding glacial deposits to a depth of a several hundred meters (Dinoloket, the Dutch open source online geodatabase, – TNO, 2021a), filling the valley with fluvioglacial deposits. These deposits (sand with clay intercalations) form the subsurface of the Bourtangermoor (Berendsen and Stouthamer, 2008; Vos et al., 2020; TNO, 2021b).

### 2.2. Study design

Based on the assumption that present-day seepage mimics historic seepage fluxes (in amount and spatial distribution), present-day groundwater data was used. Historic bog iron ore locations and their peat types were then compared with our present-day seepage

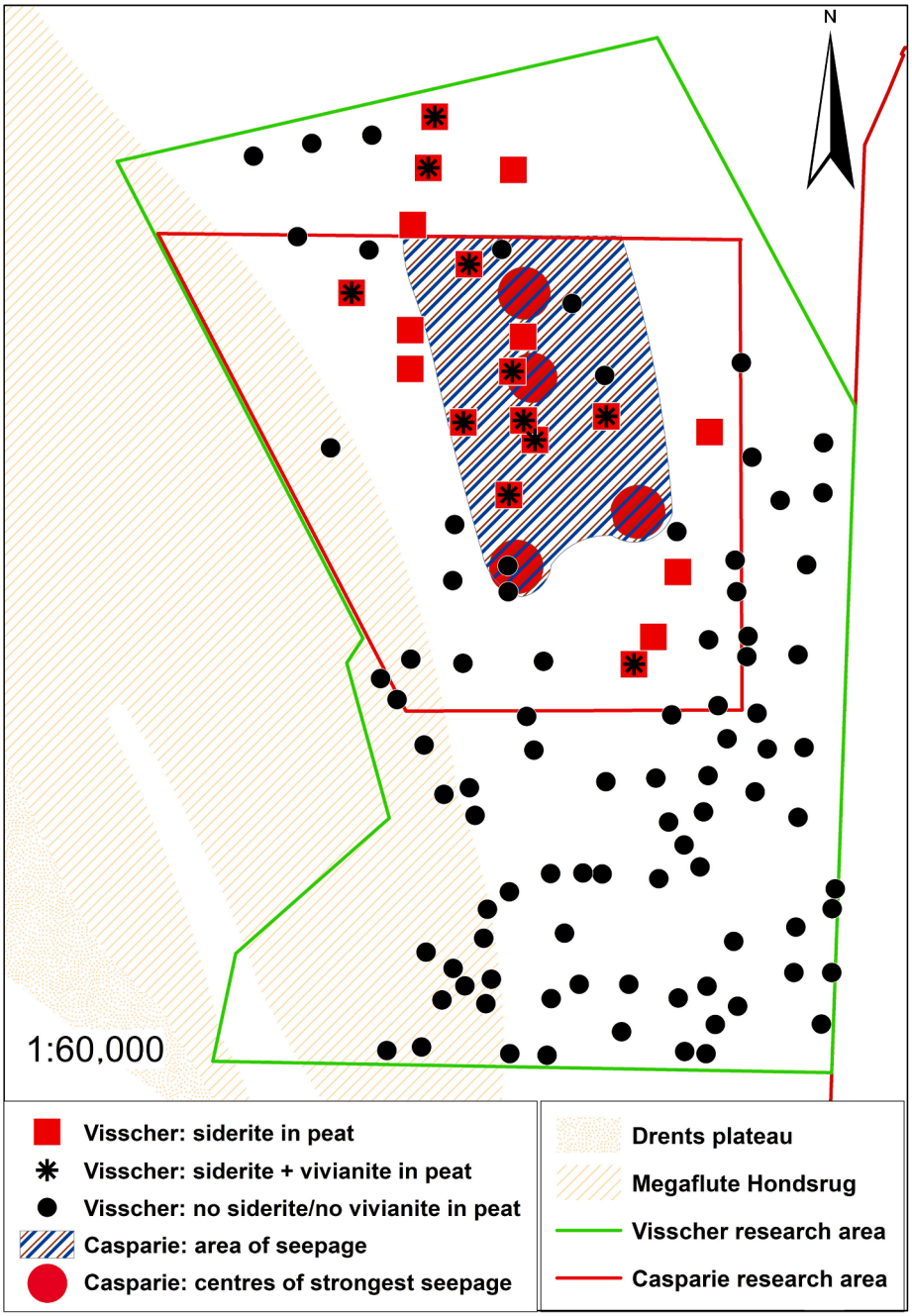


**Fig. 2.** Historic bog iron ore data of the Bourtangermoor as found in Visscher's (1931) description of peat profiles ands Casparie's (1972, 1980), description of an area of iron-rich groundwater-fed peat and centres of strongest seepage.

calculations to determine their potential relation. Relevant historic maps and literature data not available in a GIS-format, were manually digitised and georeferenced. As little original Bourtangermoor raised bog is left, this study relied heavily on an indirect line of inquiry, combining present-day seepage calculations with historic data (literature and maps) from research performed when parts of the raised bog were still intact. The historic information available spanned a period of over 120 years, from the late 19th century up to the 1970′s, describing research performed during the final stages of peat cutting. The oldest maps available were from the 1930′s and 1940′s.

Historic literature (Visscher, 1931; Casparie, 1972) was used to determine the depth of the bog iron ores in the peat column and the peat types the bog iron ores were associated with. In line with literature (Booy, 1986; Knibbe, 1969; Berendsen and Stouthamer, 2008), we assumed that glauconite in the shallow marine sands of the Breda Formation (the geohydrological base) is the source of iron in the Pleistocene cover sands and hence groundwater (TNO, 2021b). Alternative sources of iron (e.g. microbial activity) were not considered in this research. Furthermore was assumed that iron was uniformly distributed in the source rocks and that iron was present in sufficient amounts not to be a limiting factor in the depositions of bog iron ores (Zoeteman, 1970; Schaeffer, 1976).

For this research, we used literature written in English, Dutch, German and French. Peat terminology, especially terminology of groundwater-fed peat, proved to be not consistent in different languages. The distinction between rainwater-fed peat (i.e. raised bog) and groundwater-fed peat, however, was always clear. For this reason we limited ourselves in terminology to peat being either groundwater-fed or rainwater-fed.

### 2.3. Present-day seepage flux calculations

Seepage is only possible when two conditions are fulfilled: (1) the deeper aquifer must have a higher hydraulic head than the shallower aquifer (i.e. the difference in piezometric water levels between both aquifers is negative); and (2) there must be some interaction between both aquifers to allow seepage. We used groundwater data from Dinoloket (TNOb,c) to locate areas with negative differences in piezometric water levels between aquifers. Calculating the differences in piezometric water levels was done with data modelled according to groundwater model NHI 3.0 (Hoogewoud et al., 2010; Bus and Zaadnoordijk, 2018), the model then available. A new model, NHI 4.0, was introduced in 2022 (Hunink et al., 2019), however, without a full description of methods. We therefore decided to do the calculations with both models to compare the results, but used the NHI 3.0 model to analyse the possible relation between present-day seepage and historic bog iron ores, given that that model was fully published.

NHI 3.0 has seven aquifers defined in the study area, NHI 4.0 eight. The draft report of model 4.0 (Hunink et al., 2019) does not explain this change, but does mention that the new model was developed to improve modelling of shallow groundwater processes. We therefore assumed that the extra aquifer was inserted in the shallower part of the subsurface. Both models cover the subsurface down to the geohydrological basis formed by marine clays of the Oosterhout Formation, lying approx. 50 m below mean sea level (msl) (=60–65 m below ground surface) in the southeast of the research area, dipping to approx. 140 m below msl (which is ground surface here) in the northwest.

March 2017 was selected to analyse present-day seepage and March 1980 to assess seepage patterns prior to large-scale landscape interventions (e.g. groundwater withdrawal for industrial activities, construction of new suburbs) of the past decades. Groundwater data from the 1950′s – prior to the large-scale land consolidations – would have been more representative of historic conditions, but were not used due to the limited amount of measuring points at that time (TNO, 2021c). The months used represented comparable weather conditions with average to slightly above average precipitation at the end of the winter half year (KNMI, 2021), thus reducing the possible impact of the dry summer season. We did our calculations for March 2017 using both models, analysed the results of NHI 3.0 and used the results of NHI 4.0 to compare both models. We made calculations for March 1980 (model NHI 4.0 as NHI 3.0 was no longer available) to identify the possible impact of large-scale land reparcelling and groundwater extraction in the past decades.

Isohypse-data of the aquifers were recalculated into digital depth models, using the default geostatistical settings of ArcGIS. These models were snapped and resampled for equal cell size and alignment of the cells in order to produce the most accurate calculations (Price, 2016). Areas with a negative difference in piezometric water level were defined as areas of possible seepage.

The actual seepage flux (m/day) was calculated according to Bot (2016):

$$q = \frac{H_1 - H_2}{c}$$

Where: $q$ = seepage flux (m per day); $H_1$ and $H_2$ = piezometric water level of the aquifers (m), and $c$ = vertical permeability (days). Vertical permeability $c$ was calculated using:

$$c = \frac{D}{k}$$

Where: $D$ = thickness of the aquitard (i.e. clay layer) (data from TNO, 2021a); $k$ = resistance (m per day – data from Hoogewoud et al., 2010; Van der Gaast et al., 2015). However, as the thickness of the clay layer proved difficult to determine, we had to adjust our method, which is explained in the Results (Section 3.1.2).

### 2.4. Bog iron ores in historic literature and maps

#### 2.4.1. Literature

The available literature was limited to the southern part of the Bourtangermoor where peat digging took place roughly during the first six decades of the 20th century (see Fig. 1). The dissertations of Visscher (1931) and Casparie (1972) formed our main source of information. Both give extensive and detailed descriptions of peat pits or transects of peat profiles being dug during their research (Box 1). Visscher (1931) limited himself to the description of the peat profiles – peat type, thickness, mineral subsoil, bog iron ores and their position in the peat – without interpreting the relationship between these parameters. Casparie's research (1972) was done while peat digging occurred on an industrial scale, making hundreds of meters of dug out peat profiles available to him. Given the small print of the maps in his thesis (the originals are not accessible), his work provided a less accurate source than Visscher's dissertation. Other historic literature on the Bourtangermoor were only of limited value as that either did not provide original data (Van Heuveln, 1956), or only described a few isolated bog iron ore deposits (Van Bemmelen, 1895; Van Bemmelen et al., 1900; Reinders, 1902).

#### 2.4.2. Historic maps

Historic geological and soil maps were used to identify bog iron ore deposits in the original Bourtangermoor. The first geological map of The Netherlands (W.C.H. Staring, 1837) did not indicate bog iron ores. Its scale – 1:200,000 – was unsuitable for indicating smaller deposits such as bog iron ores and mapping focussed primarily on agriculture purposes (Reijers, 2012). The second geological mapping campaign (Tesch, 1945, scale 1:50.000, conducted between the 1930′s and 1945) did show bog iron ores and identified different peat types. We used Tesch (1945) to compare historic bog iron ore deposits with our present-day seepage calculations. The third mapping campaign (starting in the 1960 s, TNO, 2021d) did show bog iron ores, but were of limited use, as only one map (nr. 17 – Emmen) was published. The remaining part of the Bourtangermoor was never published on paper, and digital maps are not

**Box 1**
Historic research data used

Visscher's (1931) and Casparie's (1972) research areas – our main sources of historic literature – largely overlapped as that part of the Bourtangermoor was then being reclaimed (see Fig. 1 for the location of both research areas). Consequently only this area could be used to compare our recent seepage patterns with.

Visscher (1931) described 110 peat faces, of which two were not used due to incomplete data (see Fig. 2). Siderite ($Fe_2CO_3$) was described as the main Fe-mineral, with accessory vivianite [$(Fe_3(PO_4)_2{\cdot}8H_2O$]. The classic bog iron ore minerals goethite and limonite were only described as secondary minerals, formed through oxidation of siderite and vivianite when the peat faces were exposed to air during peat cutting. Of the 108 complete profiles, siderite is present in 20 peat faces (=19%); of these 20, vivianite is present in 12 (=60%) (vivianite was only found associated with siderite, never as the sole iron mineral (Fig. 2 and Table 1). It is important to realize that raised bogs grow on top of groundwater-fed peat (Succow and Joosten, 2001; Jansen and Grootjans, 2019; Quik et al., 2022, 2023). With increasing peat thickness, sphagnum mosses will grow, feeding on rainwater, and a raised bog develops. Visscher (1931) described siderite and vivianite only in the lower –groundwater-fed – part of the raised bog. Two peat faces had siderite lenses in a dryer interval on top of the groundwater-fed peat, but still below the raised bog. However, both descriptions showed inconsistencies in the bog iron ore position. Of the 20 profiles with siderite, 17 (85%) had a groundwater-fed peat thickness of over 1 m, 3 (15%) of up to 1 m thick. In 10 peat faces (50%) siderite was described in the top part of the groundwater-fed peat, in one (5%) throughout the groundwater-fed peat; for the remaining 9 peat faces (45%) this information was not given. The height of the Pleistocene subsurface covered with peat with siderite varied between 11.95 and 14.40 m+msl; the Pleistocene subsurface covered with peat faces without siderite deposits varied between 11.00 and 20.40 m+msl (Table 1). Taking the top of the groundwater-fed peat as the highest possible position of siderite deposition (not taking setting due to dewatering into account), siderite was deposited at a maximum height of 15.75 m above msl. Not all of Visscher's peat faces contained groundwater-fed peat; they were all on higher grounds, with raised bog developed directly on top of the Pleistocene subsurface and did not contain siderite.

Casparie did not provide individual descriptions of peat faces in his thesis (Casparie, 1972), but combined his data into profiles. Consequently a spatial analysis using individual peat faces was not possible. The maps in Casparie et al. (1980) provided additional information regarding early peat development and the spatial distribution of his seepage centres. Based on vegetation he distinguished two types of groundwater-fed peat: 'seepage peat' (i.e. peat fed by groundwater with extensive seepage) enriched in iron, and 'fen peat' (i.e. peat fed by groundwater without seepage) without iron enrichment. We restricted our terminology to groundwater-fed peat with or without iron enrichment. In the nearly 500 peat faces Casparie examined, he found siderite and vivianite as the only two Fe-minerals present, in groundwater-fed peat (his 'seepage peat', Fig. 2), and not in the raised bog op top of the groundwater-fed peat. The iron lenses he described were restricted to the top half of the groundwater-fed peat, symmetrical in shape, 0.5–10 m wide and 0.2–1 m thick.

Bog iron ores on Tesch's geological map and the post-WWII soil maps were used to compare our present-day seepage patterns with. Tesch's map (made 1930–1945), represented the extension of the Bourtangermoor during Visscher's research (Visscher, 1931), but predated Casparie's (1972); Casparie's research area, however, fell within Visscher's research area and peat cutting was still actively pursued. We assumed, therefore, that Tesch's map is also representative of the Bourtangermoor during Casparie's research. The soil maps post-dated Visscher's research by at least 20 years, as mapping took place from 1950 until the 1970's. As a number of map sheets were remapped in later years, the soil maps are less representative of the period when (parts of) the Bourtangermoor still existed.

available in sufficient detail.

Regarding soils, the oldest soil map of the Netherlands (Acker Stratingh, 1837), covered the province of Groningen, but did not show bog iron ores due to its small scale. The first detailed soils maps with bog iron ores mapped were post-World War II, when most of the Bourtangermoor was already lost to peat cutting (Stichting voor Bodemkartering, 1984). As no older soil maps were available, we used this map to compare it with the bog iron ore deposits on Tesch's geological map and our present-day seepage calculations.

#### 2.4.3. Accuracy of maps

As indicated in Section 2.1, historic maps were manually digitized and georeferenced. The accuracy of georeferencing Tesch's map was calculated using the root mean square error of the displacement vectors as given by Arcmap (Esri, 2022), added to the possible geodetic distortion occurring at the corners of the maps. The error caused by georeferencing varied between 4 and 22 m, with a mean of 15 m. As Tesch's map was composed of nine separate maps, the accuracy will vary locally. Geodetic distortion was taken to be negligible, based on the discussion and conclusions of Quik and Wallinga (2018) on georeferencing historic maps of just 35 km southwest of our research area. The bog iron ores on Tesch's map were digitized by manually encircling the area with bog iron ores. As these deposits were mapped as isolated symbols, the error difficult to quantify, but we assume it to be within the georeferencing accuracy. The accuracy of digitizing Visscher's and Casparie's maps was estimated using the size of Casparie's maps published in his thesis, as these maps were the smallest in print and his original field maps were not available. The average thickness of the lines on his maps represents a width of 35 m. Taking the same possible error for georeferencing the maps, the total estimated error adds up to 70 m.

## 3. Results

### 3.1. Seepage calculations

#### 3.1.1. Areas of possible seepage (Fig. 3)

To identify areas of possible seepage, we calculated the difference in piezometric water levels (i.e. hydraulic heads) of the aquifers identified in groundwater models NHI 3.0 and 4.0 for March 2017 and March 1980 (TNO, 2021b,c). Areas with negative differences in piezometric water levels (i.e. where the hydraulic head of the lower aquifer is higher than that of the higher aquifer) were identified as areas of possible seepage (for seepage flux calculations and actual seepage values, see Section 3.1.2). Our analysis showed two different patterns of possible seepage: one related to shallow aquifers (the aquifers above aquifer 4 in NHI 3.0; above aquifer 5 in NHI 4.0) and one related to deep aquifers (the aquifers below aquifers 5 in NHI 3.0; below aquifer 6 in NHI 4.0). The aquifers were separated by a clay layer (Urk Formation in our research area), situated at a depth of 20–40 m below msl (ground surface is 10–15 m above msl) in the southeast to close to mean sea level (approx. ground surface) in the northwest (Hoogewoud et al., 2010; TNO, 2021a). Areas with negative differences in hydraulic head are further referred to as seepage areas (see section 3.1.2 for uncertainties in the flux calculations, and the supplement for the calculations done with all

aquifers).

Both models are consistent in producing different patterns for shallow and deep seepage, but disagree on the extent of seepage and the source of seepage (i.e., either from shallow or deep aquifers). NHI 3.0 showed shallow seepage throughout the Bourtangermoor with the exception of the southern boundary, while shallow seepage in NHI 4.0 was limited further to the north of the Bourtangermoor (Fig. 3, top figures). Both models showed deep seepage in the areas with historic data, but disagree on the source of seepage north of the research area along the foot of the Hondsrug (Fig. 3, bottom figures). Where NHI 3.0 assigned all three areas to deep aquifers, NHI 4.0 assigned only the southernmost area to deep seepage, but the two areas to the north to shallow seepage. The seepage patterns for March 2017 and March 1980 (both NHI 4.0) showed comparable seepage patterns for shallow and deep aquifers, albeit with differences in piezometric water levels and the extent of areas of possible shallow seepage (Fig. 3).

### 3.1.2. *Seepage flux calculations (Fig. 4)*

Calculating actual seepage fluxes (see Section 2.2) in the research area proved difficult. The area with historic data is situated at the foot of the megaflute Hondsrug, where the subsurface is tectonically complex due to glacial activity (Berendsen and Stouthamer, 2008). The clay layer separating shallow and deep aquifers is folded and fractured, resulting in a layer that varies in thickness over short distances or is even missing

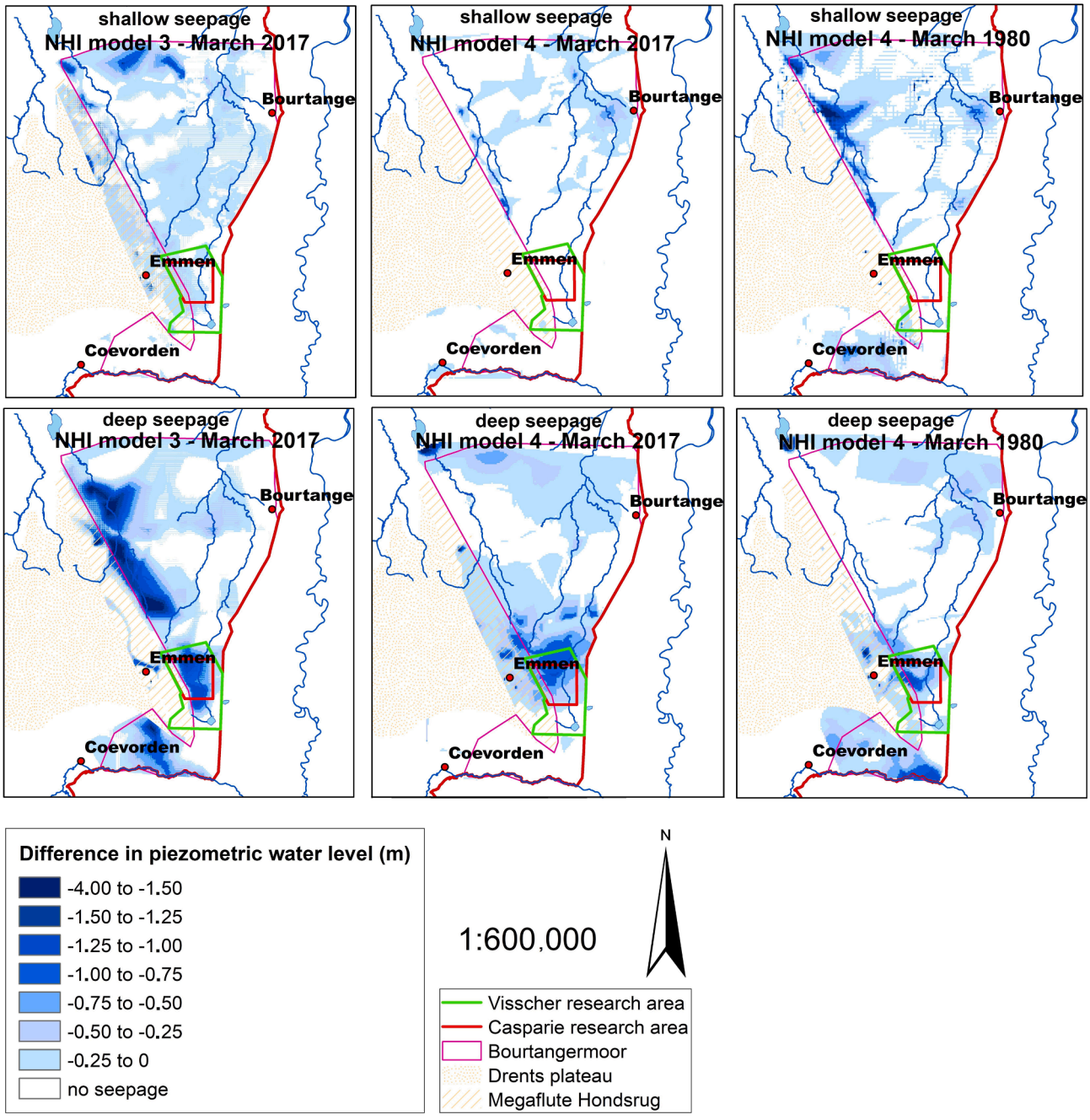


**Fig. 3.** Present-day seepage patterns. See text for a discussion on the use of the term seepage for differences in piezometric water level. Top figures: Seepage from shallow aquifers calculated with NHI model 3 (March 2017 – left), NHI model 4 (March 2017 – middle) and NHI model 4 (March 1980 – right). Bottom figures: Seepage from deep aquifers calculated with NHI model 3 (March 2017 – left), NHI model 4 (March 2017 – middle) and NHI model 4 (March 1980 – right). A complete set of calculations for the three models can be found in the Supplement. Legend: The differences in piezometric water level between -4 m and -1.50 m are represented by one colour as they were only found locally.

(TNO, 2021b), making standard seepage flux calculations not possible. To be able to estimate present-day seepage fluxes, we calculated a theoretical clay layer using cores from the Dinoloket geodatabase (TNO, 2021b - see Fig. 4). We added up the thicknesses of all clay layers in the cores from the top of the core to a depth of 30 m below msl (the estimated depth of the only continuous clay layer in the subsurface – TNO, 2021c) and divided it through the total amount of cores in the area (Table 2). This resulted in a theoretical clay layer of 1,9 m, evenly spread out over the area. Using this thickness and clay characteristics from Van der Gaast et al. (2015), we calculated seepage values of 0.63 and 0.22 cm/day for a difference in waterhead height of 200 cm (larger differences were only very locally found) and 0.47 and 0.17 cm/day for a difference in waterhead height of 150 cm (see Table 2). Bot (2016) defined seepage over 0.5 cm/day as strong seepage. Aggenbach et al. (2021) calculated seepage fluxes up to 0.96 cm per day in seepage peat, with the highest seepage values close to valley slope. Our calculated present-day seepage fluxes are lower, but are only an estimate. The cores are not evenly distributed over the area, making the estimated average thickness inaccurate. It is also uncertain how representative our theoretical clay layer is for actual seepage, as groundwater will follow the path of least resistance. As is not possible in our study area to calculate exact – location-specific – seepage fluxes, we used the term 'seepage' for areas with negative differences in piezometric levels.

### 3.1.3. *Historic bog iron ores related to present-day shallow seepage patterns (Fig. 5)*

A visual analysis of the shallow seepage pattern (calculated with NHI model 3.0 – see section 2.3) and historic siderite bog iron ore deposits (Visscher, 1931; Casparie, 1972), did not reveal an obvious relation (Fig. 5A). None of Visscher's (1931) 20 peat faces with siderite bog iron ores (red squares and black stars) fell within an area of strongest shallow seepage (dark blue colours). Ten peat faces (50 %) lay within an area of minor shallow seepage (light blue), five (25 %) at the edge of minor seepage or infiltration, and five (25 %) in an area of infiltration (white).

Casparie (1972) described two groundwater-fed peat types at the base of the raised bog: one not enriched in iron (his non-ferruginous fen peat), and one enriched in iron (his ferruginous or iron-rich seepage peat). He defined three areas of extensive seepage (Casparie, 1972; Casparie et al., 1980 – red circles in Fig. 5A), and a wider area of iron-rich peat with siderite bog iron ores (hatched area). Comparing his data with our present-day shallow seepage, it is evident that his iron-rich seepage peat falls outside any area of strong shallow seepage. Half of his

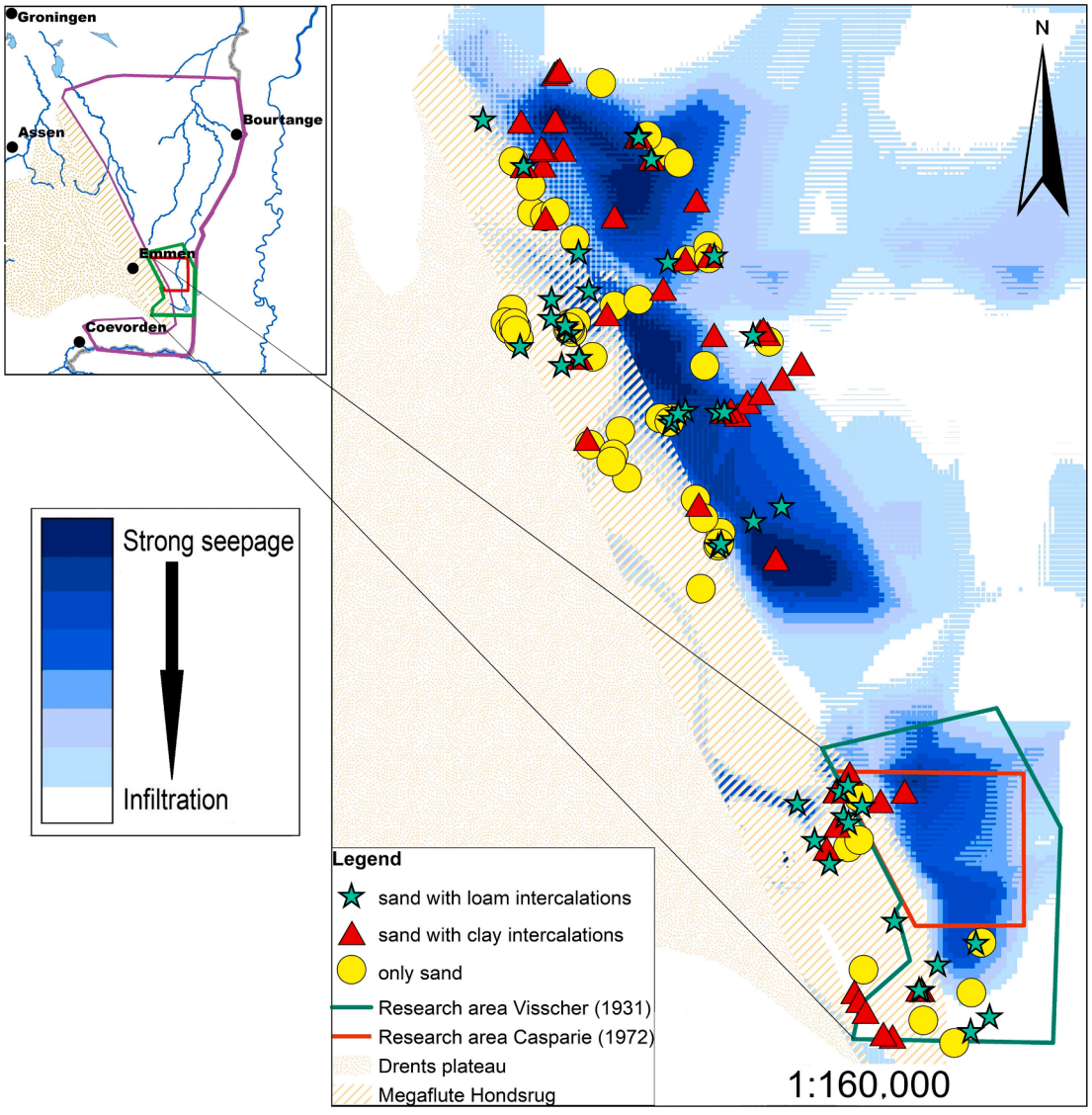


**Fig. 4.** The cores used for seepage flux calculations (data from TNO, Dinoloket, 2021b). The cores have a minimum depth of 30 m below msl. If deeper, only the top 30 m is used for the calculations. Cores are mostly composed of sand; symbols indicate intercalations of loam or clay. For accurate values of differences in piezometric water level, see Fig. 3.

**Table 1**
Summary of the peat faces characteristics in Visscher (1931).

| **Total number of peat faces** | 108 | |
|---|---|---|
| **Peat faces with siderite** | 20 (of which 12 with accessory vivianite) | |
| **Thickness of rainwater-fed peat (Sphagnum peat) related to the presence of siderite in the lower groundwater-fed part of the raised bog** | | |
| *Thickness (m)*[*,**,***] | *Siderite present* | |
| 0 – 1.00 | 20 % | 4 (of 20) |
| 1.00 – 2.00 | 35 % | 7 |
| 2.00 – 3.00 | 40 % | 8 |
| 3.00 – 4.00 | 5 % | 1 |
| **Thickness of groundwater-fed peat (fen peat, seepage peat) related to the presence of siderite** | | |
| *Thickness (m)* | *Siderite present* | |
| 0.10 – 1.00 | 15 % | 3 (of 20) |
| 1.00 – 2.00 | 75 % | 15 |
| 2.00 – 2.05 | 10 % | 2 |
| *Position of siderite in groundwater-fed, lower part of the raised bog* | | |
| Throughout | 5 % | 1 (of 20) |
| Top | 50 % | 10 |
| Not given | 45 % | 9 |
| **Maximum elevation of siderite in peat column** | | |
| (height of Pleistocene subsurface plus top groundwater-fed peat; height in m above MSL) | | |
| 13.55 – 14.00 *m* | 10 % | 2 (of 20) |
| 14.00 – 15.00 *m* | 60 % | 12 |
| 15.00 – 15.75 *m* | 25 % | 5 |
| Height not given | 5 % | 1 |
| **Height of Pleistocene subsurface for:** | | |
| Peat profiles with siderite | 11.95 – 14.40 m | |
| Peat profiles without siderite | 11.00 – 20.40 m | |
| * | Visscher's two sphagnum peat layers ('Older' and 'Younger' sphagnum peat) are merged here. | |
| ** | Thickness is of dewatered peat. | |
| *** | Thickness probably does not represent full thickness in a number of profiles due to peat reclamation. | |

seepage peat falls within an area of less extensive shallow seepage, half in an area of present-day infiltration. Unfortunately, we cannot be more specific as Casparie's descriptions of separate peat faces were not available and we had to rely on his small figures. However, all data provided by Casparie (1972) and Visscher (1931) agree regarding the lack of relation between siderite deposits in the raised bog and present-day shallow seepage.

Both historic maps available – Tesch's geological map and the soil map (both 1:50,000) – only show bog iron ores along natural streams. The siderite bog iron ores as described in the Bourtangermoor historic literature are not on the maps. The most extensive classic-type bog iron ore deposits are found along streams in the eastern and southern part of the raised bog (Fig. 5B, C). The streams at the foot of the Hondsrug (light-brown hatched area) showed only a few patches of bog iron ore deposits, mainly north of our area with historic data. Bog iron ores on the soil map were far more extensive than on Tesch's map in the Bourtangermoor, with the exception of our research area where bog iron ores on Tesch's map were far more abundant (see Fig. 5B, C). A possible explanation is that Tesch's map was made when both research areas were, at least partly, still intact, making his map more accurate than the more recent soil map that was made when the area was already destroyed by peat digging. This apparent inconsistency does not change that the visual overlap between historic classic-type bog iron ores along natural streams and present-day shallow seepage patterns is limited.

### *3.1.4. Historic bog iron ores related to present-day deep seepage patterns (Fig. 6)*

Comparing our present-day deep seepage patterns with historic literature, we found that Visscher's (1931) peat faces with siderite all fell within an area of extensive present-day deep seepage (Fig. 6A). Of these, 75 % (15 of 20) were in an area of strong present-day deep seepage (dark blue); four lay at the fringes of that area (20 %). One peat face lacked location information. All peat faces with both siderite and vivianite were in an area of strong deep present-day seepage. Of the peat faces without siderite, 17 % (15 of 88) lay in an area of strong present-day deep seepage (dark blue colours), 17 % (15 of 88) along its fringes (light-blue colours), 60 % (53 of 88) in an area of infiltration (white – see Table 1 for additional information on peat types and peat thicknesses). Zooming in on Casparie (1972), his ferruginous to iron-rich groundwater-fed peat (his only peat type with siderite) and our present-day deep seepage patterns showed visually a good overlap. His iron-rich groundwater-fed peat fell within an area of extensive present-day deep seepage(Fig. 6A). Fourteen of Visscher's peat faces fell within Casparie's area of iron-rich groundwater-fed peat. Of these nine contained siderite (64 %).

Comparing present-day deep seepage with historic maps, it was evident that the classic-type bog iron ores on Tesch's geological map and the soil map showed limited affiliation to present-day deep seepage (Fig. 6B). The streams along the foot of the megaflute Hondsrug (light brown hatched zone) show only a few scattered patches of bog iron ores in the southern and central areas of strong present-day deep seepage, but did show classic-type bog iron ores in the northern area of strong present-day deep seepage. The abundant, classic-type bog iron ore deposits along the natural streams further to the east lay outside any area of present-day deep seepage. Comparing both historic maps with present-day deep seepage patterns, the only relation between classic-type bog iron ores and present-day deep seepage in the Bourtangermoor is found in the northern area of present-day deep seepage.

**Table 2**
Seepage calculations, using cores with a minimum depth of 30 m below msl.

| | | |
|---|---|---|
| Total amount of cores | 112 | |
| Cores with only sand | 57 | |
| Cores with clay layers# | 55 | |
| Total thickness of clay layers in all cores | 213 m | |
| Thickness of clay when evenly distributed over area (= total thickness of all clay layers divided by total number of cores = 213/112) | 1.90 m | |
| $k_{clay1}$* | 0.60 cm/day | |
| $k_{clay2}$* | 0.21 cm/day | |
| $c_{clay1}$ = av. thickness clay divided by $k_{clay1}$ | 316 days | |
| $c_{clay2}$ = av. thickness clay divided by $k_{clay2}$ | 904 days | |
| Difference in piezometric water level used | 2.00 and 1.50 m | |
| **Seepage flux** | | |
| Difference in water head height ($H_1$ - $H_2$ | 2.00 m | 1.50 m |
| Seepage flux for clay 1 | 0.63 cm/day | 0.47 cm/day |
| Seepage flux for clay 2 | 0.22 cm/day | 0.17 cm/day |

# Loam is reduced to 1.3% (sandy loam) to 15 % (loess) of its original thickness when recalculated to clay. As most loam in the cores is sandy, loam layers are ignored in these calculations (Biron, 2004).
* Depending on type of clay; see Van der Gaast et al. (2015).

Equations used for seepage:

$$c = D/k$$

$$q = (H_1 - H_2) / c$$

Where:
$H_1$, $H_2$: piezometric water level of the aquifers (m)
$c$: vertical permeability (days)
$D$: thickness of clay layer (m)
$k$: resistance (cm/day)
$q$: seepage flux (cm/day)

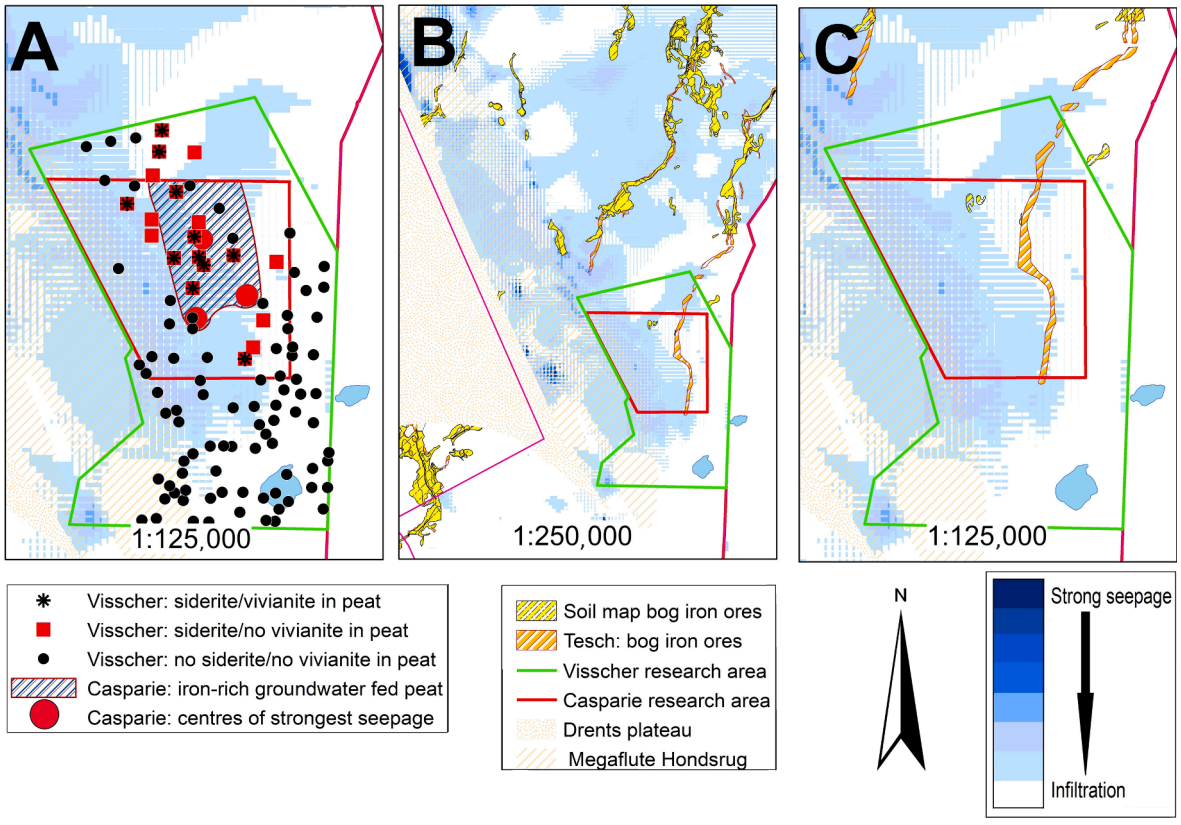


**Fig. 5.** Shallow seepage compared to historic bog iron ore data. (A) Compared to siderite bog iron ores as described by Visscher (1931) and Casparie (1972, 1980). (B) Compared to bog iron ores on Tesch's geological map (Tesch, 1945) and the soil map (Stichting voor Bodemkartering, 1984). (C) Compared to bog iron ores on Tesch's map and the soil map in the historic research areas.

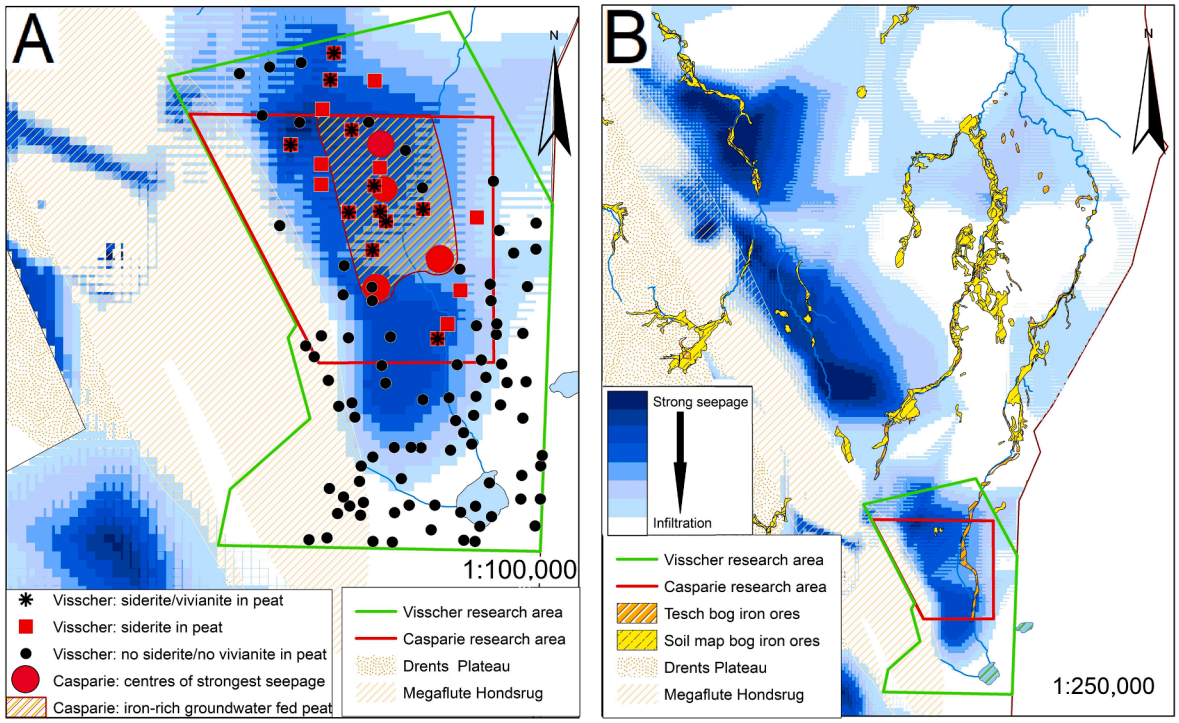


**Fig. 6.** Pattern of present-day deep seepage compared to historic bog iron ore data. (A) Compared to Visscher (1931) and Casparie (1972, 1980). (B) Compared to Tesch's geological map (Tesch, 1945) and the soil map (Stichting voor Bodemkartering, 1984).

## 4. Discussion

### *4.1. Comparing groundwater models NHI 3.0 and NHI 4.0 (Figs. 7 and 8)*

We analysed the relation between historic bog iron ores and present-day seepage using groundwater model NHI 3.0 (Hoogewoud et al., 2010; Bus and Zaadnoordijk, 2018). We also did the calculations with NHI model 4.0 that came available during this research (Hunink et al., 2019) for comparison. We found remarkable differences between both models. Model 4.0 predicted shallow seepage in a much larger area of the Bourtangermoor than model 3.0 (Fig. 7), with deep seepage limited to the southern part (Fig. 8). Focussing on the area along the foot of the Hondsrug, seepage from shallow aquifers was limited to non-existent in NHI 3.0, but extensive in NHI 4.0 (Fig. 7). Seepage from deep aquifers in the southern area was extensive in both models, but where NHI model

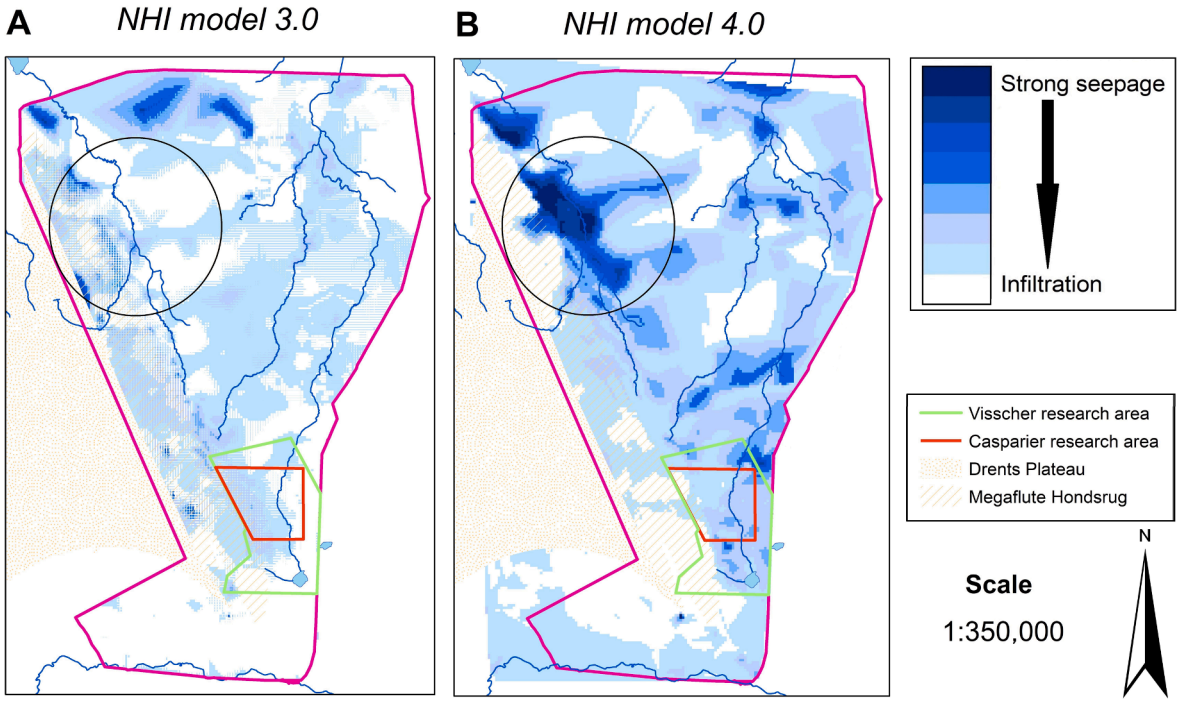


**Fig. 7.** Present-day shallow seepage patterns (March 2017) calculated with (A) Groundwater model NHI 3.0. (B) Groundwater model NHI 4.0. The two black circles point to large differences in the two groundwater models along megaflute the Hondsrug.

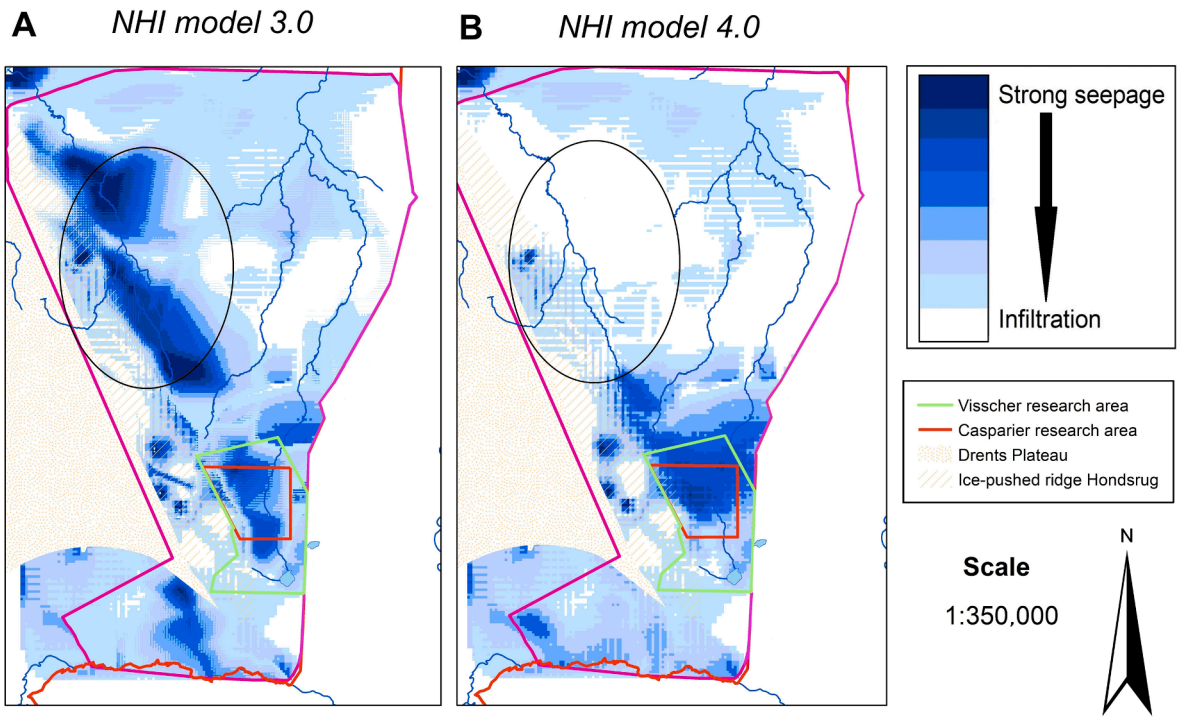


**Fig. 8.** Present-day deep seepage patterns for March 2017 calculated with (A) Groundwater model NHI 3.0. (B) Groundwater model NHI 4.0. Deep seepage is found along the foot of the ice-pushed ridge Hondsrug from south to north in model NHI 3.0, but is limited to the southern part using model NHI 4.0. The largest differences between both models – along megaflute the Hondsrug – are encircled.

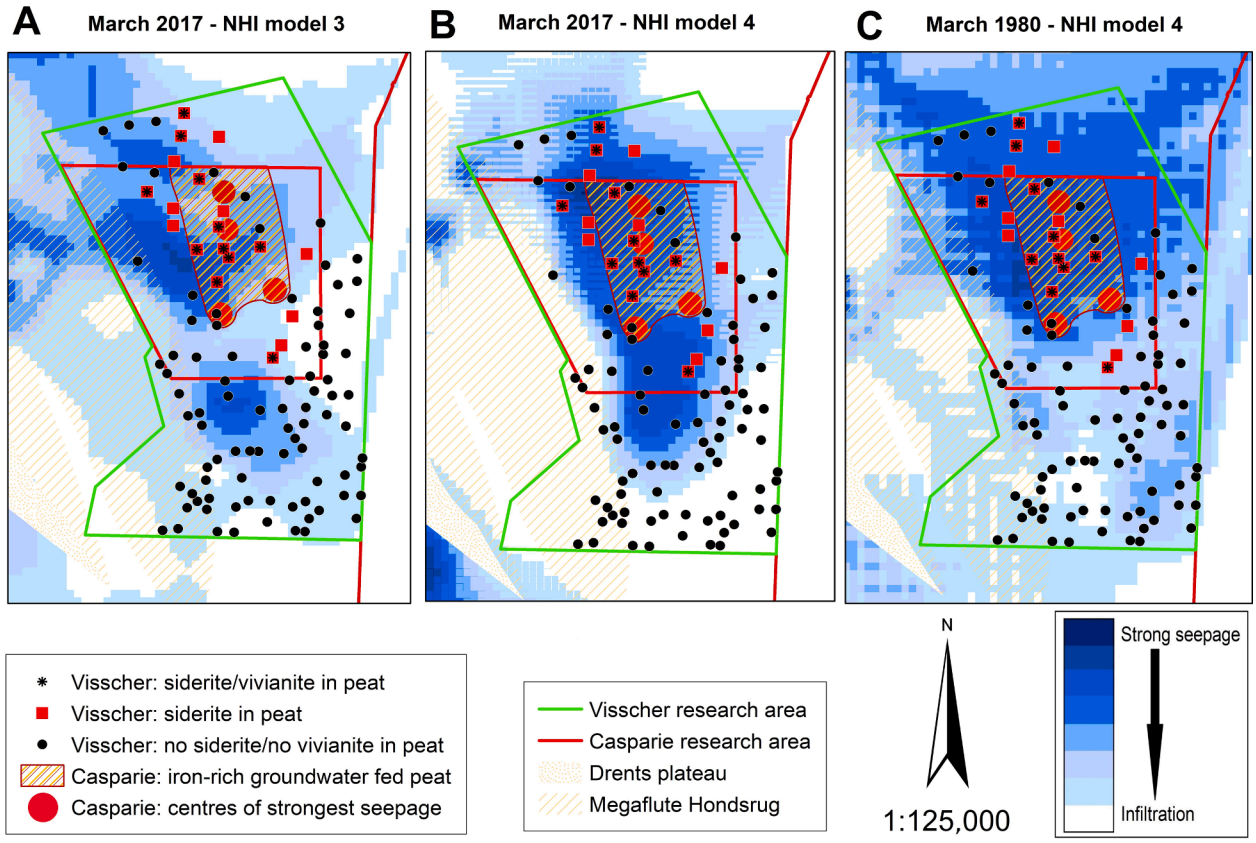


**Fig. 9.** Present-day deep seepage patterns compared to historic data (Visscher, 1931; Casparie, 1972, 1980). (A) March 2017, calculated with NHI model 3.0. (B) March 2017, calculated with NHI model 4.0. (C) March 1980, calculated with NHI model 4.0.

3.0 gave extensive deep seepage along the foot of the Hondsrug from south to north, NHI model 4.0 only predicted extensive deep seepage in the southern area, but not towards the north (Fig. 8). Both models agreed in the area with historic data, where they showed identical patterns of present-day deep seepage both in extent and in differences in piezometric water levels (Fig. 9). Both models showed a good relation between siderite bog iron ores and strong present-day deep seepage with a 75 % overlap, as did our calculations for March 1980 (Fig. 9C), indicating that large-scale interventions, such as reparcelling, new-built suburbs or industrial activity during the last decades did not have major impact on the deep seepage pattern. As historic data on siderite bog iron ores were only available in the area where both models agree, we cannot use them to discuss the differences in the two groundwater models.

However, groundwater from deep aquifers is anaerobic; iron will be present as $Fe^{2+}$, which is soluble in water. As deep groundwater can be hundreds to thousands of years old, there is ample time to accumulate iron. The iron content of deep groundwater can be up to 30 mg/l (Bot, 2016); iron in groundwater extracted from below the only clay layer in the subsurface in the eastern part of the Bourtangermoor varies between 11 and 25 mg/l (Steinweg et al., 2018). Shallow groundwater contains on average between 0,5 and 1 mg/l of iron (Bot, 2016). Groundwater from shallower aquifers is younger (weeks to years) and therefore had less time to accumulate iron. Shallower groundwater will – especially in the phreatic zone – contain oxygen, oxidising $Fe^{2+}$ to $Fe^{3+}$ which is insoluble and will be deposited as Fe(oxy)hydroxides. Groundwater extracted from shallow aquifers in the northern area of the Hondsrug, the area where the two groundwater models differ, contains 5 mg/l iron (De Vries, 2019), higher than the average iron content for shallow groundwater. Historic maps Tesch, 1945; Stichting voor Bodemkartering, 1984) showed large classic-type bog iron ore deposits in that area (Fig. 6B), indicating strong seepage. Both models agree on the presence of seepage, but disagree on the depth. The high iron content in shallow groundwater in this area could be caused by mixing of deep and shallow seepage in the lagg (the edge) of the raised bog. The lagg water flowed towards the northwest, providing the iron for the extensive classic-type bog iron ores along the stream. The flow of iron-rich seepage water through the lagg along the Hondsrug towards the northwest could possibly contribute to the discrepancies between the two groundwater models (Fig. 8).

### 4.2. Present-day seepage related to historic bog iron ores in the Bourtangermoor

Classic-type bog iron ore were (and still are) found in the shallow Pleistocene subsurface along natural streams and in low-lying areas (Steur et al., 1991). Siderite bog iron ores were found exclusively in the lower, groundwater-fed peat of the raised bog, concentrated in the top part of the groundwater-fed peat (Visscher, 1931; Casparie, 1972). Present-day seepage in the Bourtangermoor showed two distinct patterns: one of the aquifers above the only continuous clay layer in the subsurface (our shallow seepage) and one of the aquifers below this clay layer (our deep seepage). The Bourtangermoor siderite bog iron ores (Visscher, 1931; Casparie, 1972) showed a good visual fit with present-day deep seepage (Fig. 6A). There was, however, an eastward shift of approximately 500 m with the areas of strongest present-day deep seepage. Part of this shift could be explained by regional hydrology and geology. The regional flow direction of groundwater is to the northeast (TNO, 2021c). The horizontal displacement of the seepage would roughly be two to three times the vertical distance the seepage had to travel (Bot, 2016), resulting in a horizontal displacement of roughly 60 to 90 m. A second factor to consider would be the complex fractured and folded local geology that made it impossible to pinpoint exact locations of maximum seepage (Section 3.2.1).

Of far greater importance would be the growth of groundwater-fed peat leading to filled in depressions and subsequently overgrown ridges, eventually developing into a raised bog. With the growing bog, the position of the contact zone between peat and mineral subsoil (the lagg) will change both horizontally and vertically) (Jansen and Grootjans, 2019; Sevink et al., 2022). In the lagg, water from the raised bog, shallow seepage from the Hondsrug and deep seepage diverted to the lagg by the weight of the growing bog would collect, resulting in a zone with a specific vegetation, but also in a zone where bog iron ores could be deposited. Shallow seepage would supply $HCO_3^-$ preventing the water to become acid (TNO, 2021b), deep seepage would supply iron (11–25 mg/l; Steinweg et al., 2018) With the changing lagg location, locations of bog iron ores would change through time, making a direct comparison between present-day deep seepage and historic bog iron ores complex. The diversion of deep seepage to the lagg in our research area could explain the layer on top of the seepage peat showing desiccation cracks, indicating dryer conditions as described by Casparie (1972).

### 4.3. Position of siderite bog iron ores in peat

The maximum height of the Pleistocene subsurface of peat with siderite bog iron ores was 14.40 m above msl; of peat without ores 20.40 m above msl (Table 1). This suggested that topography was one of the factors determining the development of seepage peat and hence the deposition of siderite bog iron ores, but not the limiting factor as peat with and without siderite bog iron ores were found at the same Pleistocene subsurface elevations. The co-existence of peat with and without siderite at the same height in the peat could be explained by deep seepage finding its way through the fragmented clay layer in the subsurface, resulting in specific areas where deep seepage could flow through more easily. However, the changing position of the lagg during the development of the raised bog would also have resulted in the deposition of peat with siderite bog iron ores next to peat without siderite deposits. The weight of the growing bog would be the factor determining the flow path of deep seepage, forcing seepage to the lagg and thereby determining the location of siderite bog iron ores. Siderite bog iron ores are therefore not an indication of the start of peat formation. Deposition of the ores was determined by the position of the lagg, which changed over time with the development of the bog.

### 4.4. Siderite: Primary or secondary?

Literature – local and international – is unambiguous about the relation between classic-type bog iron ores and seepage. Historic literature of the Bourtangermoor confirmed this relation for siderite bog iron ores, as they were found only in peat fed by seepage (Visscher, 1931; Casparie, 1972). Siderite ($Fe_2CO_3$) and vivianite [$Fe_3(PO_4)_2{\cdot}8H_2O$] are known as accessory minerals in the lower (anaerobic) part of classic-type bog iron ores (Knibbe, 1969; Booy, 1986; Kaczorek et al., 2004; Thelemann et al., 2017), and as small, isolated lenses in bogs (Postma, 1980). The Bourtangermoor siderite bog iron ores are unique in their size with lenses up to 10 m in circumference and thicknesses of up to 2 m (Van Bemmelen et al., 1900; Casparie, 1972). Postma (1980) mentioned siderite bog iron ores of those dimensions, but referred to Bourtangermoor researchers, suggesting that this reference could be specifically related to the Bourtangermoor.

The previous section (section 4.3) discussed the deposition of siderite bog iron ores in the lagg, where deep seepage (source of iron) and shallow seepage from the megaflute Hondsrug (source of $HCO_3^-$ preventing lagg water to become acid) could provide conditions suitable for siderite deposition. However, classic-type bog iron ores of similar size are described in this area (Booy, 1986) and in the western part of the Netherlands (Stuurman, 2008). Iron-reducing bacteria in an anaerobic water-rich environment are able to reduce up to 30 % of goethite present (Liu et al., 2011; Maitte et al., 2015; Li et al., 2022), but descriptions of classic-type bog iron ores being completely converted to siderite bog iron ores were not found in literature. Casparie's original descriptions could have provided evidence for this theory if he had described Fe-

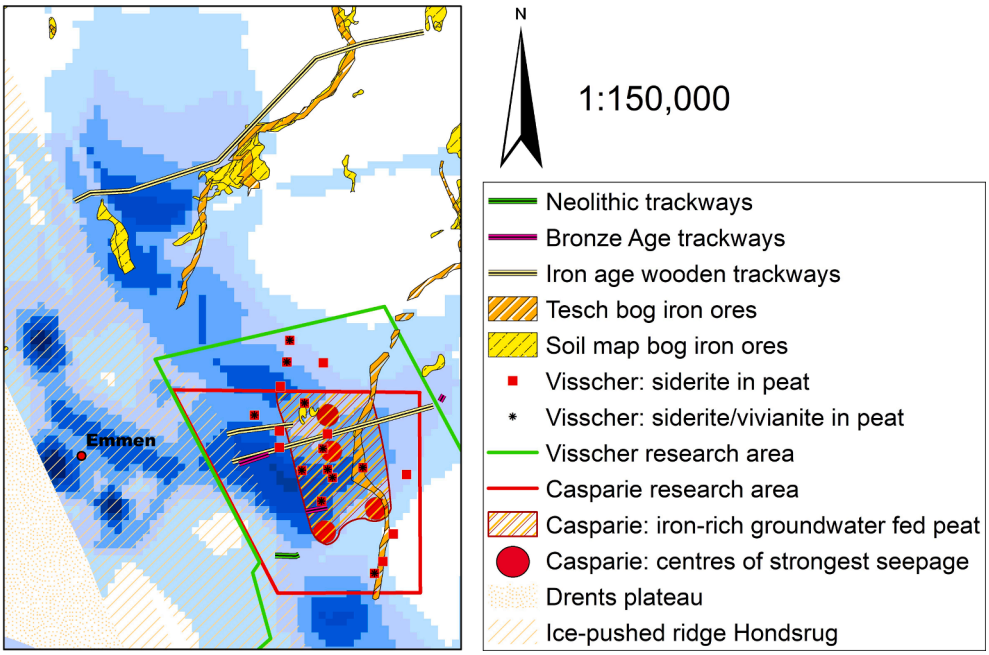


**Fig. 10.** Wooden trackways found during peat reclamation (Casparie, 1986; Casparie et al., 2004) compared to present-day deep seepage.

(oxy)hydroxides still present in the centre of the siderite/vivianite lenses. Unfortunately his descriptions were not available to us, nor are they found in literature. The favourable conditions found in the lagg for the deposition of siderite and the lack of evidence regarding the possibility of a complete conversion of goethite to siderite by bacteria, made us strongly lean towards siderite being of primary origin.

### 4.5. Importance of bog iron ores in wetland restoration

Bog iron ores could be important in their ability to extract phosphate from the environment, thereby contributing to the nutrient-poor conditions necessary for the restoration of wetlands. However, seasonal changes in groundwater level have a severe impact on the capture of phosphate by Fe-minerals. Vivianite (Fe-phosphate) is stable under anaerobic conditions. When exposed to air (with dropping groundwater level), a number of its $Fe^{2+}$-ions oxidize, converting the same number of $H_2O$-molecules to $(OH)^-$, but phosphate does remain confined in the mineral (Chiba et al., 2016; Rothe et al., 2016). However, phosphate sorbed to Fe-(oxy)hydroxides will be released when $Fe^{3+}$ will be reduced to $Fe^{2+}$ with rising groundwater levels and thus anaerobic conditions (Herndon et al., 2019; Barczok et al., 2023). The ability of bog iron ores to withdraw phosphate from the environment could be important in restoring degraded wetlands (Heiberg et al.,2012; Walpersdorf et al., 2013). However, this does not offer a simple solution as rising groundwater levels result in the release of phosphate back to the environment.

High amounts of iron are toxic for many plants and limit the development of the vegetation as only a limited amount of plant species is resistant to high iron contents in water (Casparie, 1972; Aggenbach et al., 2013). Furthermore, iron could affect the accumulation of peat, as it can oxidize organic matter to inorganic C when reduced to $Fe^{2+}$ (Middleton et al., 2006; Aggenbach et al., 2013). As iron has a profound effect on peat development, it is important to know the source of seepage, as the amount of iron in deep groundwater is much higher than that shallow groundwater (0.5–1 mg/l versus max. 30 mg/l; Bot, 2016).

### 4.6. Usefulness of Bourtangermoor bog iron ores for past societies

Classic-type bog iron ores have been an important source of iron from prehistoric times to well into the 20th century (Groenewoudt and van Nie, 1995; Thelemann et al., 2017). They are found close to the surface, are easy to recognize and collect and depleted locations could be re-used as the iron ores continued to be deposited. Wooden trackways found in the Bourtangermoor during peat digging have been the subject of discussion for past decades whether they could have been constructed for mining bog iron ores (Casparie, 1986; Casparie et al., 2004). Iron became an important metal from the Late Iron Age. Three Iron Age trackways were found (Fig. 10). Two cut across areas of present-day strong seepage and extended beyond classic-type bog iron ores along natural streams in the raised bog. These deposits would have been inaccessible as the Bourtangermoor had almost reached its maximum extend in that period (Vos et al., 2020). This is corroborated by the lack of archaeological finds from Roman times to the early Medieval period (Dans Data Station Archaeology, 2023; NAD Nuis, 2023). As siderite bog iron deposits were covered by the raised bog, there is no argument for these deposits to be either known or mined. As wooden trackways from all periods extended into areas with bog iron ores from both types, a religious connotation could be possible as lightning was known to strike bog iron ores (Booy, 1986; folk stories), leaving settlements safer from fires and its inhabitants grateful to a higher power.

## 5. Conclusions

Based on the analysis of present-day seepage data to reconstruct historic bog iron ore sites in the Bourtangermoor, a former raised bog in the north of the Netherlands, our conclusions were:

Present-day seepage from deep aquifers proved to be a good indicator for the reconstruction of historic siderite bog iron ores in the Bourtangermoor.

Present seepage from shallow aquifers did not show a relation to either historic siderite bog iron ores or classic-type bog iron ores in the Bourtangermoor.

Siderite bog iron ores do not represent the start of peat formation. The location of the lagg (changing during peat development) was the deciding factor for deposits of the ores.

The source of seepage (and thus the amount of iron) is an important factor to consider as iron can have positive and negative effects on wetland restoration.

## CRediT authorship contribution statement

**Aukjen A. Nauta:** Formal analysis, Methodology, Writing – original draft. **Roel Dijksma:** Formal analysis. **Jasper H.J. Candel:** Formal analysis. **Cathelijne R. Stoof:** Supervision.

## Declaration of competing interest

The authors declare that they have no known competing financial interests or personal relationships that could have appeared to influence the work reported in this paper.

## Data availability

Data will be made available on request.

## Acknowledgements

This research is part of the Home Turf Project of Wageningen University and Research, an interdisciplinary study on the raised bogs in the Netherlands, focussing on their development and man-land relations in the widest possible sense: from the practical use of raised bogs (foraging, growing food, peat cutting) to cultural and religious perspectives. The project was funded by NWO (Dutch Organisation for Scientific Research, Vidi Project, no. 276-60-003). Valuable discussions with colleagues from Home Turf and the Soil Science Group are greatly appreciated. The critical remarks of two anonymous reviewers were greatly appreciated. Special thanks to emeritus-professor Jan Sevink (University of Amsterdam), Ingrid Lubbers (SGL, Wageningen) and Jan Graven (Deep BV) for their discussions and suggestions. Many thanks also to environmental artist Kate Foster for her inspiring views on peatlands, bringing art and science together.

## Appendix A. Supplementary data

Supplementary data to this article can be found online at https://doi.org/10.1016/j.catena.2024.107847.

## References

Acker Stratingh, G. 1837. Bodemkaart van Nederland.
Aggenbach, H., Emsens, W.J., Grootjans, A.P., Lamers, L.P.M., Smolders, A.J.P., Stuyfzand, P.J., Wolejko, L., van Diggelen, R., 2013. Do high iron concentrations in rewetted rich fens hamper restoration? Preslia 85 (3), 405–420.
Aggenbach, C.J.S., Van Loon, A., Ferrario, I., Van Diggelen, R., Nijp, J.J., Van der Sande, M., Buis, K., 2021. Waterhuishouding van grondwatergevoede beekdalvenen: ontwikkeling, bepalende factoren en mogelijkheden voor herstel. VBNE, Vereniging van Bos- en Natuurterreineigenaren, Driebergen, pp. 179–pp.
Anderson, W.F., 1962. Ijzeroer. Grondboor En Hamer 16 (2), 56–63.
Baird, A.J., 2009. Carbon cycling in northern peatlands. DC, American Geophysical Union, Washington.
Barczok, M., Smith, C., Di Domenico, N., Kinsman-Costello, L., Singer, D., Herndon, E., 2023. Infuence of contrasting redox conditions on iron (oxyhydr)oxide transformation and associated phosphate sorption. Biogeochemistry 166, 87–107.
Berendsen, H.J.A., Stouthamer, E., 2008. Landschappelijk Nederland: de fysisch-geografische regio's. Van Gorcum, Assen, p. 240.
Biron, D.J., 2004. Beter bouw- en woonrijp maken: Een verkennend onderzoek naar het bouw- en woonrijp maken in de Nederlandse praktijk en de problematiek rond wateroverlast op de bouwplaats. Delft University of Technology, MSc-thesis, p. 256.
Bönsel, A., Sonneck, A.-G., 2011. Effects of a hydrological protection zone on the restoration of a raised bog: a case study from Northeast-Germany 1997–2008. Wetl. Ecol. Manag. 19 (2), 183–194.
Booy, A.H., 1986. IJzeroer in Drenthe. Ontstaan, voorkomen, winning en gebruik. Nieuwe Drentse Volksalmanak 103, 12.
Bot, B., 2016. Grondwaterzakboekje. Bot Raadgevend Ingenieur, 465 pp.
Bourtangermoor (2021). Natuurpark Bourtangermoor. www.naturpark-moor.eu.
Bragazza, L., Buttler, A., Siegenthaler, A., Mitchell, A.D., 2009. Carbon Cycling in Northern Peatlands. In: Baird, A.J., Belyea, L.R., Comas, X., Reeve, A.S., Slater, L.D. (Eds.), Am. Geophys. Union vol. 184.
Bus, S., Zaadnoordijk, W.J., 2018. Handleiding Grondwatertools. Geologische Dienst Nederland - TNO 22.
Casparie, W.A., 1972. Bog development in Southeastern Drenthe (the Netherlands). Vegetatio 25, 272 pp.
Casparie, W.A., 1986. The two Iron Age wooden trackways XIV (Bou) and XV (Bou) in the raised bog of Southeast Drenthe (the Netherlands. Palaeohistoria 169–210.
Casparie, W.A., Brakke, J., Stil, H., Van der Hoek, S., 1980. Het veen – natuurlijk en menselijk moeras. Provinciaal Museum Drenthe, Assen, p. 72.
Casparie, W.A., Van Geel, B., Hanraets, A.F.M., Jansma, E., Stuijts, I.L.M., 2004. De veenweg van Nieuw Dordrecht – onvoltooid en niet gebruikt. Nieuwe Drentse Volksalmanak 114–141.
Chiba, C., Takahashi, M., Ohshima, E., Kwawamata, T., Sugiyama, K., 2016. The synthesis of metavivianite and the oxidation sequence of vivianite. J. Mineral. Petrol. Sci. 115, 485–489.
Chimner, R.A., Cooper, D.J., Wurster, F.C., Rochfort, L., 2017. An overview of peatland restoration in North America: where are we after 25 years? Restor. Ecol. 25 (2), 283–292.
Dans Data Station Archaeology (2023). KNAW archaeological database: https://archaeology.datastations.nl/.
De Vries, A., 2019. Gebiedsdossier grondwaterwinning De Groeve. Royal Haskoning 64, pp.
Emsens, W.J., Aggenbach, C.J., Smolders, A.J., Zak, D., van Diggelen, R., 2017. Restoration of endangered fen communities: the ambiguity of iron-phosphorus binding and phosphorus limitation. J. Appl. Ecol. 54 (6), 1755–1764.
Esri (2022). Fundamentals of georeferencing a raster dataset, available at http://desktop.arcgis.com/en/arcmap/10.3/manage-data/raster-and-images/fundamentals-for-georeferencing-a-raster-dataset.htm.
Groenewoudt, B.G., van Nie, M., 1995. Assessing the scale and organisation of Germanic iron production in Heeten, the Netherlands. J. Eur. Archaeol. 3 (2), 29.
Heiberg, L.B., Koch, C., Kjaergaard, C., Jensen, H.S., Hansen, J., Christian, H., 2012. Vivianite precipitation and phosphate sorption following iron reduction in anoxic soils. J. Environ. Qual. 41 (3), 938–949.
Herndon, E.M., Kinsman-Costello, Duroe, K.A., Mills, J., Kane, E.S., Sebestyen, S.D., Thompson, A.A., Wullschleger, 2019. Iron (oxyhydr)oxides serve as phosphate traps in tundra and boreal peat soils. Journal of geophysical research: Biogeosciences, 124 (2).
Hoogewoud, J., de Lange, W., Hunink, J., Vernes, R., Simmelink, E., Hummelman, J., Pastoors, R., 2010. Nationaal Hydrologisch Instrumentarium – NHI: Modelrapportage Fase 2. Deelrapport 1. Ondergronds Fase 2, 33.
Hunink, J., Walsum, P. van, Vermeulen, P., Pouwels, J., Bootsma, H., janssen, G., Swierstra, W, Prinsen, G, Meshgi, A., Veldhuizen, A., Lande, W. de, Hummelman, J., Bos-Burgering, L, Kroon, T. (2019). Veranderingsrapportage LHM 4.0 Beheer en onderhoud van het lagenmodel, het topsysteem, het bodem-water-plant-atmosfeer systeem en het oppervlaktewater. Deltares, 142 pp.
Jansen, A. and Grootjans A.P. (2019). Hoogvenen : landschapsecologie, behoud, beheer, herstel. Gorredijk, Noordboek Natuur. 392 pp.
Joosten, H., Tannenberger, Tannenberger, F., Moen, A. (2017). Mires and Peatlands of Europe. Status, Distribution and Conservation. Schweizerbart, 780 pp.
Kaczorek, D., Sommer, M., Andruschkewitsch, I., Oktaba, L., Stahr, K., 2004. A comparative micromorphological and chemical study of Raseneisenstein (bog iron ore) and Ortstein. Geoderma 121 (1), 83–94.
Kaczorek, D., Sommer, M., 2004. Micromorphology, chemistry, and mineralogy of bog iron ores from Poland. Catena 54 (3), 393.
Knibbe, M., 1969. Gleygronden in het dekzandgebied van Salland. Wageningen, Centrum voor Landbouwpublikaties en Landbouwdocumentatie.
KNMI (2021). KNMI - Archief maand/seizoen/jaaroverzichten, KNMI.
Koster, E., Favier, T., 2005. Peatlands, Past and Present. In: Koster, E.A. (Ed.), The Physical Geography of Western Europe. Oxford, Oxford University, Press, pp. 161–182.
Laine, J., 2009. Carbon Cycling in Northern Peatlands. In: Baird, A.J., Belyea, L.R., Comas, X., Reeve, A.S., Slater, L.D. (Eds.), Am. Geophys. Union, vol. 184.
Li, H., Ding, S., Song, W., Zhang, Y., Ding, J., Jie, L.u., 2022. Iron reduction characteristics and kinetic analysis of *Comamonas testosteroni* Y1: a potential iron-reduction bacteria. Biochem. Eng. J. 177, 108256.
Liu, D., Wang, H., Dong, H., Qiu, X., Dong, X., Cravotta III, C.A., 2011. Mineral transformations associated with goethite reduction by *Methanosarcina barkeri*. Chem. Geol. 288 (1–2), 53–60.
Maitte, B., Jorand, F.P.A., Grgic, D., Adbelmoula, M., Carteret, C., 2015.
McBratney A.B., Stockmann. U., Angers, D.A., Minasny B., Field D.J. (2014). Challenges for soil organic carbon research. In: A.E. Hartemink and K. McSweeney (editors): Soil Carbon. Springer: 503 pp.
Middleton, B., Grootjans, A., Jensen, K., Olde Venterink, H., & Margóczi, K. (2006). Fen Management and Research Perspectives: An Overview. In B. Beltman, R. Bobbink, J. T. A. Verhoeven, & D. F. Whigham (Eds.), Wetlands: Functioning, Biodiversity Conservation, and Restoration, 191th ed., pp. 247-268). (Ecological Studies; No. 191).
Lucassen, E.C.H.E.T., 2000. Increased groundwater levels cause iron toxicity in Glyceria fluitans (L.). Aquatic Botany (2000) 66: 321–327. Remineralization of ferrous carbonate from bioreduction of natural goethite in the Lorraine iron ore (Minette) by Shewanella putrefaciens. Chem. Geol. 412, 48–58.
Mohr, K., Suda, J., Kros, J., Brummer, C., Kutsch, W.L., Hurkuck, M., Woesner, E., Wesseling, W., 2015. Atmosphärische Stickstoffeinträge in Hochmoore Nordwestdeutschlands und Möglichkeiten ihrer Reduzierung – eine Fallstudie aus einer landwirtschaftlich intensiv genutzten Region. Johann Heinrich Von. Thünen-Institut.
NAD Nuis, 2023. Noordelijk Archeologisch Depot. https://www.nadnuis.nl/.
Nichols, J.E., Peteet, D.M., 2019. Rapid expansion of northern peatlands and doubled estimate of carbon storage. Nat. Geosci. 12 (11), 917–921.

Paulissen, M., 2023. Cultural sponges. Past and present uses, meanings and legacy of raised bogs in the Low Countries. Wageningen University and Research, p. 197 pp.. PhD thesis.
Postma, D., 1980. Formation of siderite and vivianite and the pore-water composition of a Recent bog sediment in Denmark. Chem. Geol. 31, 225–244.
Price, M.H., 2016. Mastering ArcGIS, McGraw-Hill. Education 448 pp.
Quik, C. and Wallinga, J. (2018) Reconstructing lateral migration rates in meandering systems – a novel Bayesian approach combining optically stimulated luminescence (OSL) dating and historical maps. Earth Surface Dynamics 6 (2018) 3.2023.
Quik, C., Palstra, S.W.L., Beek, van, R., Velde, van der, Y., Candel, J.H.J., Linden, van der, M., Kubiak-Martens, L., Swindles, G.T., Makaske, B., 2022. Dating basal peat: The geochronology of peat initiation revisited. Quat. Geochronol. 72. https://www.sciencedirect.com/science/article/pii/S1871101422000267.
Quik, C., Van der velde, Y., Candel, J.H.J., Steinbuch, L., Van Beek, R., Wallinga, J., 2023. Faded landscapes: unravelling peat initiation and lateral expansion at one of northwest Europe's largest bog remnants. Biogeosciences 20, 695–718. https://bg.copernicus.org/articles/20/695/2023/bg-20-695-2023-discussion.html.
Reijers, T., 2012. Emerging sciences and their impact (1780–1877). Dutch Earth Sciences - Development and Impact. P. Floor. The Hague, Royal Geological and Mining Society of the Netherlands, p. 273.
Reinders, G. (1902). Mededeeling omtrent de verspreiding van het deels poedervormig deels pijpvormig ijzeroer in de provinciën Groningen en Drenthe. Mededeelingen omtrent de geologie van Nederland, verzameld door de commissie voor het geologische onderzoek. Amsterdam, Koninklijke Akademie van Wetenschappen. 31: 18 pp.
Rothe, M., Kleeberg, A., Hupfer, M., 2016. The occurrence, identification and environmental relevance of vivianite in waterlogged soils and aquatic sediments. Earth Sci. Rev. 158, 51–64.
Schaeffer, C.O., 1976. Grondwater, kwaliteit en kwetsbaarheid. H Twee o: Tijdschrift Voor Watervoorziening En Afvalwaterbehandeling 9 (19), 354–358.
Schouten, M.G.C. (2002). Conservation and restoration of raised bogs : geological, hydrological and ecological studies. Dublin, Dúchas -The Heritage Service of the Department of the Environment and Local Government.
Schwertmann, F., 1992. Iron Minerals in Surface Environments. Catena Suppl. 21, 7–30.
Sevink, J., Van der Linden, M., Jansen A.J.M., 2022. Peatland restoration based on a landscape (palaeo)ecological system analysis (LESA): the case of Aamsveen, eastern Netherlands. Mires and Peat, 28, article 23, 16 pp.
Shotyk, W., 1988. Review of the inorganic geochemistry of peats and peatland waters. Earth Sciences Reviews 25, 95–176.
Steinweg, C., Holsteijn, A.L., Van den Brink, C., 2018. Gebiedsdossier grondwaterwinning Sellingen. Royal Haskoning, DHV, p. 44.
Stichting Bargerveen (2021). Bargerveen Foundation. www.stichting-bargerveen.nl.
Steur, G.G.L., Heijink, G., De Bakker, H., Boersma, O.H., Hamming, C., 1991. Bodemkaart van Nederland, schaal 1:50000 : algemene begrippen en indelingen. Wageningen, Staring Centrum.
Stichting voor Bodemkartering, 1984. De bodemkaart van Nederland 1:50000. Wageningen, Stiboka.
Stuurman, R., 2008. Brokken oerbank in zandzuiger van een HSL bouwput bij Hazerswoude. Grondboor & Hamer 6, 126–129.
Succow, M., Joosten, H., 2001. Landschaftsökologische Moorkunde. Schweitzerbart'sche Verlagsbuchandlung 622 pp.
Tesch, P. (1935-1945). Geologische kaart van Nederland.
Thelemann, M., Bebermeier, W., Hoelzmann, P., Lehnhardt, E., 2017. Bog iron ore as a resource for prehistoric iron production in Central Europe — A case study of the Widawa catchment area in eastern Silesia, Poland. Catena 149 (Part 1), 474–490.
TNO, Geological Survey of the Netherlands (2021a). DGM: Digital Geological Model of the Netherlands. https://www.dinoloket.nl/digitaal-geologisch-model-dgm.
TNO, Geological Survey of the Netherlands (2021b). Dinoloket. Data van de Nederlandse Ondergrond. https://www.dinoloket.nl/.
TNO, Geological Survey of the Netherlands (2021c). Grondwaterstanden in Beeld. https://www.grondwatertools.nl/gwsinbeeld/.
TNO, Geological Survey of the Netherlands (2021d). Geologische kaart. https://www.dinoloket.nl/geologische-kaart/.
Van Bemmelen, J.M., 1895. Over de samenstelling, het voorkomen en de vorming van sideroze (witte klien) en van vivianiet in de onderste darglaag der hoogveenen van Zuidoost Drenthe. Amsterdam. J. Müller.
Van Bemmelen, J.M., Hoitsema, C., Klobbie, E.A., 1900. Les accumulations ferrugineuses dans et sous les tourbieres. Gisement, composition, formation. Archives Neerlandaises Des Sciences Exactes Et Naturelles, Ch. 19, 73 pp.
Gaast, van der J.W.J., Vroon, H.R.J., Massop, H.Th., L, Wesseling, J.G. (2015). Landsdekkende schematisering en parameterisatie van het topsysteem ten behoeve van hydrologische modellering. Alterra rapport 2686, Wageningen, 112 pp.
Van Heuveln, B., 1956. Minerale afzettingen in het Smeulveen. Boor En Spade 38, 16.
Virtanen, K., 1994. Geological control of iron and phosphorous precipitates in mires of the Ruukki-Vihanti area, Central Finland Espoo, Geological Survey of Finland. PhD 72, pp.
Visscher, J. (1931). Das Hochmoor von Sudost-Drente - Geomorphologisch betrachtet. Geographisch en Mineralogisch-Geologisch Instituut. Utrecht, Rijksuniversiteit Utrecht. PhD: 108 pp.
Vos, P., Meulen, van der M., Weerts, H., Bazelmans, J., 2020. Atlas of the Holocene Netherlands, landscape and habitation since the last ice age. Amsterdam University Press.
Walpersdorf, E., Bender Koch, C., Heiberg, L., O'Connell, D.W., Kjaergaard, C., Bruun Hansen, H.C., 2013. Does vivianite control phosphate solubility in anoxic meadow soils? Geoderma 193–194, 189–199.
Yu, Z., Beilman, D.W., Jones, M.C., 2009. In: Baird, A.J., Belyea, L.R., Comas, X., Reeve, A.S., Slater, L.D. (Eds.), Carbon Cycling in Northern Peatlands, vol. 184. American Geophysical Union.
Zoeteman, B.C.J., 1970. Zuiveringsmethoden van zoet grondwater voor de drinkwatervoorziening. H Twee o: Tijdschrift Voor Watervoorziening En Afvalwaterbehandeling 3 (3), 44–53.